



Identifying Control Targets for Regulating Mild Cognitive Impairment Using Reduced Computational Models of a Life Kinetic Network

UGBENE, I. J.^{1,*} , AGWEMURIA, R. O.² 

^{1,2}Department of Mathematics, Federal University of Petroleum Resources, Effurun

ARTICLE INFO

Received: 10/08/2023
Accepted: 01/12/2023

Keywords

Attractor states;
Control sets,
Experiment modeling
cycle, Mild cognitive
impairment (MCI),
Network reduction

ABSTRACT

Network reduction, which emphasized preserving feedback loops, identified potential ways to regulate dynamics in a computational model of mild cognitive impairment (MCI). Control sets capable of modulating MCI-associated attractors were identified in the full and reduced networks, though fewer in the latter. While the reduced size conferred a computational advantage, further validation is needed to determine the physiological relevance and translatability of proposed targets. Results demonstrate preserved dynamical features relevant for identifying and modulating MCI attractors despite network reduction, suggesting potential for data-driven intervention strategies. However, rigorous experimental validation and refinement through iterative experiment-modeling cycles will be essential for rigorously evaluating and progressively shaping in silico predictions into mechanism-based MCI therapies.

1. INTRODUCTION

Mathematical modeling approaches that rely on network analysis are becoming increasingly essential for understanding complex neurological conditions like MCI (Zhang, et al, 2008). Boolean network models are particularly useful because they can capture high-level dynamical features related to cognitive function, such as network attractors (Choi, et al, 2012). However, the size of neural networks reconstructed from data can pose computational challenges in identifying and interpreting attractor dynamics (Schwab et. al., 2012). To address this, we propose a network reduction technique that effectively reduces the size of a large Boolean network reconstructed from the ISAAC aging study (Kaye, et al, 2011), while still preserving stable feedback loops and dynamical features.

Our approach relies on the work of Veliz-Cuba et al. (Veliz-Cuba et al, 2014). We

find that the reduced network still captures similar attractor basin distributions as the full network, indicating preservation of relevant dynamics (Shreim et. al, 2010). We then apply the caspo_control software package (Videla et. al., 2017) to efficiently search for control targets within the reduced network, identifying nodes whose perturbation modifies MCI-associated attractors. Our findings demonstrate the potential of dynamical network reduction approaches as a computational method for modeling and regulating complex conditions like MCI (Strogatz, 2001). By preserving features relevant for phenotype of interest while reducing network size, we may create more tractable yet biologically faithful models to identify novel intervention points (Qiu et. al., 2021). Further experimental validation is needed to assess the efficacy of our proposed control targets for regulating MCI-related

*Corresponding author, e-mail:ugbene.ifeanyi@fupre.edu.ng

DIO

©Scientific Information, Documentation and Publishing Office at FUPRE Journal

attractor dynamics in vivo (Chen et. al., 2020).

2. MATERIALS AND METHODS

A Boolean network S which is of size n , i.e composed of n genes, is a collection of n Boolean local transition functions such that $F = (s_i: S_2^n \rightarrow S_2, s_i(y) \rightarrow y_i), i \in \{1, \dots, n\}$ where y denotes a configuration of S , and y_i denotes the state of gene i (Kauffman, 1969)

The state of the network at any given time step is determined by the Boolean transition functions associated with each variable. These transition functions can be represented as Boolean functions $s_i: \{0,1\}^n \rightarrow \{0,1\}$ which defines how the future value of the i -th variable depends on the present values of the other variables. Mathematically, the Boolean transition function s_i can be expressed as follows:

$$s_i: (s_1, s_2, \dots, s_n) \mapsto s'_i$$

Here, (s_1, s_2, \dots, s_n) represents the current state of all variables, and s'_i represents the updated value of the i -th variable in the next time step.

The transition function s_i can be defined using logical operation such as *AND* (\wedge), *OR* (\vee), and *NOT* (\neg) on the input variables s_1, s_2, \dots, s_n . These logical relationships capture the regulatory relationships between the variables and determine how they influence each other states.

By iterating the Boolean transitions functions over time, the Boolean network evolves from one state to another, exhibiting dynamic behavior and potentially reaching stable states or cycles. Analyzing the dynamics of Boolean networks provides insights into their behaviours, attractors, and regulatory mechanisms

Now from the reconstructed ISAAC network (Dinwoodie, 2016),

Let;

$$\begin{aligned} y_1 &= mci & y_2 &= compuse \\ y_3 &= meanws & y_4 &= numfir \\ y_5 &= numtrans & y_6 &= numwalks \end{aligned}$$

$$\begin{aligned} y_7 &= sleeplatency \\ y_8 &= sleepivroom \\ y_9 &= timeasleep & y_{10} &= ttib \\ y_{11} &= waso & y_{12} &= wscv \\ y_{13} &= wsq3 & y_{14} &= wssigma \\ y_{15} &= oohhours \end{aligned}$$

(1)

Following the above assumptions, the boolean transition function from (Dinwoodie, 2016) is as follows;

$$s_1 = (\neg y_{13} \wedge y_{11} \wedge y_2) \vee (\neg y_{13} \wedge y_8 \wedge \neg y_2)$$

$$s_2 = y_{14} \wedge \neg y_1$$

$$s_3 = (y_{14} \wedge y_{13}) \vee (y_{13} \wedge \neg y_{12})$$

$$s_4 = \neg y_{13} \vee y_8 \vee y_5$$

$$s_5 = y_4$$

$$s_6 = y_{14} \wedge \neg y_{12}$$

$$s_7 = y_{11} \wedge y_{10}$$

$$s_8 = \neg y_{10} \wedge y_9$$

$$s_9 = y_{10}$$

$$s_{10} = y_9$$

$$s_{11} = y_{10} \wedge y_7$$

$$s_{12} = y_{14} \wedge \neg y_3 \vee y_{14} \wedge y_1$$

$$s_{13} = \neg y_6 \wedge \neg y_1 \vee y_3$$

$$s_{14} = y_{12} \wedge y_3$$

$$s_{15} = \neg y_{10} \wedge y_8 \vee \neg y_{10} \wedge y_6 \vee$$

$$\neg y_{10} \wedge \neg y_4$$

(2)

The wiring diagram D of a boolean network is a directed graph, denoted as $D = (V, E)$, where V represents the set of nodes or genes, and E represents the set of directed edges or regulatory relationships. The node set V can be represented as $V = \{v_1, v_2, \dots, v_n\}$, where v_i represents the i th gene or variable in the Boolean network. The edge set E can be represented as $E = \{(v_i, v_j), : v_i \rightarrow v_j\}$, where (v_i, v_j) represents a directed edge from node v_i to node v_j , indicating a regulatory relationship where gene v_i influences gene v_j (Albert and Othmer, 2003).

The wiring diagram of the reconstructed network (Dinwoodie, 2016) is shown in Figure 1. If we give the set $\{0,1\}$ the

structure of a finite field with standard addition and multiplication, i.e., $S_2 = \{0,1\}$, then the functions $S_i : S_2^n \rightarrow S_2$ can be represented as polynomials over S_2 . Thus, the dynamical system $S = (s_1, \dots, s_n) : S_2^n \rightarrow S_2^n$ becomes a

polynomial dynamical system, as described in (Veliz-Cuba et al, 2010). This polynomial representation of Boolean networks provides a useful tool for studying their dynamics.



Figure 1: Wiring Diagram for Life Kinetics and Cognitive Impairment (see (Dinwoodie, 2016).

The process of transforming Boolean functions into polynomials in $S_2[y_1, \dots, y_n]$ is governed by the following rules: $y \wedge z = yz$, $y \vee z = y + z + yz$, $y^2 = y$, $\alpha y = 0 \forall \alpha \in \mathfrak{R}$ and $\neg y = 1 + y$, where the operations are computed modulo 2. By applying these rules to the network, we can derive the corresponding polynomial expressions.

$$\begin{aligned}
 s_1 &= (y_{11}(1 + y_{13})(1 + y_2)) + (y_8(1 + y_{13})(1 + y_2)) + (y_{11}(1 + y_{13})(1 + y_2)) + (y_8(1 + y_{13})(1 + y_2)) + y_{11}y_8(1 + y_2)(1 + y_{13}) = (1 + y_{13} + y_2 + y_{13}y_2)(y_8 + y_{11} + y_8y_{11}) \\
 s_2 &= y_{14}(1 + y_1) = y_{14} + y_1y_{14} \\
 s_3 &= y_{14}y_{13} + y_{13}(1 + y_{12}) + y_{13}y_{14}(1 + y_{12}) = y_{13} + y_{13}y_{12} + y_{12}y_{13}y_{14}
 \end{aligned}$$

$$\begin{aligned}
 s_4 &= (1 + y_{13}) + y_8 + y_5 + y_5y_8(1 + y_{13}) = 1 + y_{13} + y_5 + y_8 + y_8y_5 + y_5y_8y_{13} \\
 s_5 &= y_4 \\
 s_6 &= y_{14}(1 + y_{12}) = y_{14} + y_{14}y_{12} \\
 s_7 &= y_{11}y_{10} \\
 s_8 &= (1 + y_{10})y_9 = y_9 + y_9y_{10} \\
 s_9 &= y_{10} \\
 s_{10} &= y_9 \\
 s_{11} &= y_{10}y_7 \\
 s_{12} &= y_{14}(1 + y_3) + y_1y_{14} + y_1y_{14}(1 + y_3) = y_{14} + y_{14}y_3 + y_{14}y_1y_3 \\
 s_{13} &= (1 + y_6)(1 + y_1) + y_3 + y_3(1 + y_6)(1 + y_1) = 1 + y_1 + y_6 + y_1y_6 + y_3y_6 + y_1y_3 + y_1y_3y_6 \\
 s_{14} &= y_3y_{12} \\
 s_{15} &= y_8(1 + y_{10}) + y_6(1 + y_{10}) + (1 + y_4)(1 + y_{10}) + (y_8(1 +
 \end{aligned}$$

$$y_{10})))(y_6(1 + y_{10}))((1 + y_4)(1 + y_{10})) = 1 + y_{10} + y_8 + y_6 + y_4 + y_4y_{10} + y_8y_{10} + y_6y_{10} + y_8y_6 + y_4y_6y_8 + y_6y_8y_{10} + y_4y_6y_8y_{10} \quad (3)$$

The behavior of a dynamic Boolean network is described by the difference equation $y(t + 1) = S(y(t))$, where the dynamics are generated by iteration of S . The dynamics of S are given by the state space graph T , which is defined as the graph with vertices in $S_2^n = 0, 1^n$. The graph has an edge from $y \in S_2^n$ to $x \in S_2^n$ if and only if $x = S(y)$. The states $y \in S_2^n$ where the system will stabilize are attractors of a Boolean network and may include steady states (fixed points), where $S(y) = y$, and cycles, where $S^k(y) = y$ for some integer $k > 1$. Attractors in Boolean network modeling may represent cell types (Kauffman, et. al., 1969) or cellular states such as apoptosis, proliferation, or cell senescence (Huang, 1999) and (Shmulevich and Dougherty, 2010). Identifying the attractors of a system is an important step towards controlling the system and can be done using tools from computational algebra (Veliz-Cuba et. al., 2010) and (Veliz-Cuba et. al., 2014).

To find the steady states of the network, we need to solve the system of equations where $s_i = y_i$, for $i = 1$ to 15. This means we want to find the roots of $f_i = 0$, where $f_i = s_i - y_i$. We obtain the following system of equations:

$$\begin{aligned} f_1 &= (1 + y_{13} + y_2 + y_{13}y_2)(y_8 + y_{11} + y_8y_{11}) + y_1 = 0, \\ f_2 &= y_{14} + y_1y_{14} + y_2 = 0, \\ f_3 &= y_{13} + y_{13}y_{12} + y_{12}y_{13}y_{14} + y_3 = 0, \\ f_4 &= 1 + y_{13} + y_5 + y_8 + y_8y_5 + y_5y_8y_{13} + y_4 = 0, \\ f_5 &= y_4 + y_5 = 0, \\ f_6 &= y_{14} + y_{14}y_{12} + y_6 = 0, \\ f_7 &= y_{11}y_{10} + y_7 = 0, \\ f_8 &= y_9 + y_9y_{10} + y_8 = 0, \\ f_9 &= y_{10} + y_9 = 0, \end{aligned}$$

$$\begin{aligned} f_{10} &= y_9 + y_{10} = 0, \\ f_{11} &= y_{10}y_7 + y_{11} = 0, \\ f_{12} &= y_{14} + y_{14}y_3 + y_{14}y_1y_3 + y_{12} = 0, \\ f_{13} &= 1 + y_1 + y_6 + y_1y_6 + y_3y_6 + y_1y_3 + y_1y_3y_6 + y_{13} = 0, \\ f_{14} &= y_3y_{12} + y_{14} = 0, \\ f_{15} &= 1 + y_{10} + y_8 + y_6 + y_4 + y_4y_{10} + y_8y_{10} + y_6y_{10} + y_8y_6 + y_4y_6y_8 + y_6y_8y_{10} + y_4y_6y_8y_{10} + y_{15} = 0 \end{aligned}$$

(4)

Since the system is not linear, traditional methods like Gaussian elimination cannot be applied. However, we can utilize computational algebra to solve it by representing the solutions as an algebraic object known as an ideal of polynomials, denoted as $I = \{f_1, f_2, \dots, f_{15}\}$. By finding the Grobner basis (CoxD et al 1998) of this ideal using mathematical software tools like Sagemath (SageMath. (Version 9.2), we can obtain an equivalent but simpler representation. Finding the Grobner basis allows us to transform the original system into a more manageable form while preserving its solutions. It is a powerful technique for solving systems of polynomial equations. By computing this basis, we can obtain a set of polynomials that share the same solutions as the original system, but in a more convenient and simplified manner. The resulting simplified representation of the system can then be used to determine its solutions.

$$\begin{aligned} y_1 &= 0 & y_2 &= 0 \\ y_3 + 1 &= 0 & y_4 &= 0 \\ y_5 &= 0 & y_6 &= 0 \\ y_7 &= 0 & y_8 &= 0 \\ y_9 &= 0 & y_{10} &= 0 \\ y_{11} &= 0 & y_{12} &= 0 \\ y_{13} + 1 &= 0 & y_{14} &= 0 \\ y_{15} + 1 &= 0 \end{aligned} \quad (5)$$

Therefore, we can solve it to obtain $y = 001000000000101$ as a steady state of the network.

2.1 Network Reduction Methodology

The approach used for network reduction is an iterative method developed by (Veliz-Cuba et. al., 2014) implemented in the Pystablemotif package (Rozum et. al., 2022), which reduces the size of the network while maintaining feedback loops that encode crucial dynamical features (Veliz-Cuba et al, 2014).

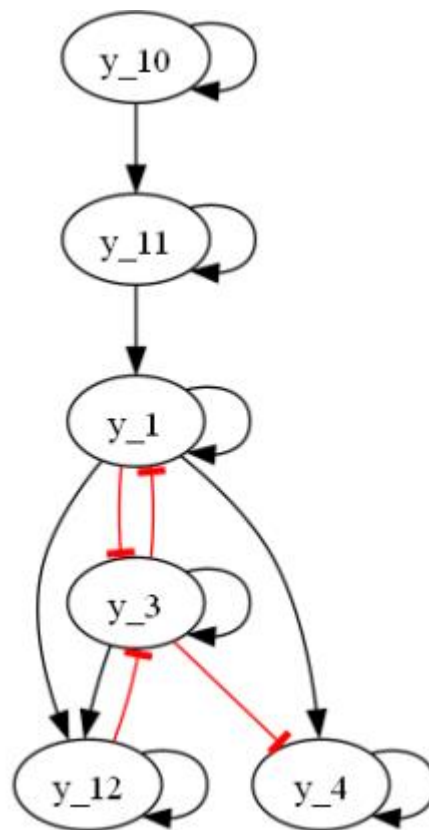


Figure 2: Wiring diagram of the reduced Life kinetics and Impairment Network

At each iteration, the edge removal that results in the smallest change in the number of loops is determined.

If this edge removal maintains a minimum number of loops, it is performed. This process is repeated until the specified percentage of edges have been removed. For this study, we applied this method to the reconstructed ISAAC network (Dinwoodie, 2016). The network consists of 15 nodes and their interactions. We specified a 70% edge reduction, while maintaining some feedback loops. This resulted in a reduced network of 6 nodes

and their edges as should in Figure 2. While network reduction can result in some loss of detail, we argue that it still captures the higher-level dynamical features crucial for the phenotype of interest (Dinwoodie, 2016) and (Saadatpour et. al., 2010). By preferentially maintaining loops hypothesized to determine functions (Albert et al, 2003), relevant attractors may still emerge.

We acknowledge that there are potential limitations to this approach, but we argue that network reduction remains a feasible

and useful first-pass, computationally efficient approach for generating testable hypotheses. More realistic models can then incorporate the lost details (Saadatpour et. al., 2010). The associated boolean transition function of the reduced network is as follows;

$$\begin{aligned} s_1 &= \neg y_3 \wedge y_1 \wedge y_{11} \\ s_2 &= \neg y_1 \wedge \neg y_{12} \vee y_3 \\ s_4 &= \neg y_3 \wedge y_1 \vee y_4 \\ s_{10} &= y_{10} \\ s_{11} &= y_{10} \wedge y_{11} \\ s_{12} &= y_1 \wedge y_3 \wedge y_{12} \end{aligned}$$

The polynomial for the transition function becomes;

$$\begin{aligned} s_1 &= y_1 y_{11} (1 + y_3) = y_1 y_3 y_{11} + y_1 y_{11} \\ s_3 &= ((1 + y_1)(1 + y_{12})) + y_3 + \\ & y_3((1 + y_1)(1 + y_{12})) = y_1 y_3 y_{12} + \\ & y_1 y_3 + y_1 y_{12} + y_1 + y_3 y_{12} + y_{12} + 1 \\ s_4 &= y_1(1 + y_3) + y_4 + y_1 y_4(1 + y_3) = \\ & y_1 y_3 y_4 + y_1 y_3 + y_1 y_4 + y_1 + y_4 \\ s_{10} &= y_{10} \\ s_{11} &= y_{10} y_{11} \\ s_{12} &= y_1 y_3 y_{12} \end{aligned}$$

(7)

Since its nonlinear we use the groebner basis earlier said to reduce and solve, using the mathematical software Sagemath (SageMath. (Version 9.2), Computer software, 2021), the solution to the above system was obtained to be;

$$\begin{aligned} y_1 &= 0 & y_3 + 1 &= 0 \\ y_4 &= 0 & y_{10} &= 0 \\ y_{11} &= 0 & y_{12} &= 0 \end{aligned}$$

(8)

Hence the steady state of the reduced network is $y = 010000$. Hence the reduction technique used preserved the steady state.

In this study, we have employed computational algebra to discover the steady states of complex networks.

Specifically, we have used Boolean algebra to model the network dynamics and identify the attractors, which correspond to the steady states of the system. Additionally, we have reduced the size of the network using the (Veliz-Cuba et. al., 2014) method, which preserves the feedback loops that encode crucial dynamical features of the system.

There are also other software tools available for computing the steady states (attractors) of Boolean networks. One such tool is BoolNet, which is a R-based package for analyzing Boolean networks (Mussel et. al., 2010). Another tool is PyBoolNet, which is a Python package for analyzing and visualizing the dynamics of Boolean networks (Klarner et. al., 2017).

In summary, while we have used computational algebra and the (Veliz-Cuba et. al., 2014) method for discovering steady states and reducing network size, there are also other software tools available for analyzing Boolean networks. Researchers can choose the tool that best meets their needs based on factors such as ease of use, computational efficiency, and available features.

2.2 Identifying Control Targets and Attractor Analysis in Full and Reduced Network

This section focuses on identifying potential control targets within the full and reduced network models. Two computational tools, *caspo_control* (Videla et. al., 2017) and *pystablemotif* (Rozum et. al., 2022), were leveraged to systematically analyze the attractor landscape and identify control targets (Samaga et. al., 2009). These tools can also calculate the network's stable states (attractors) (Samaga et. al., 2009), their corresponding basins of attraction (Samaga et. al., 2009), and potential intervention points (control targets) that can switch the network from one attractor to another (caspo, 2017), (Rozum et. al., 2022) and (Samaga et. al., 2009). In the previous section, computational algebra

(6)

techniques were employed to determine the network’s steady state expression profiles (Gunawardena, 2014), other steady states (attractors) of the full and reduced network where determined using an asynchronous update scheme in Boolnet

(Mussel et al ,2010). Seven (7) attractors were obtained, six (6) of the attractors has mci to be 0 (OFF), that is it prevents mci and the remaining one has mci = 1, which is the abnormal attractor as shown in Figure 3 and 7.

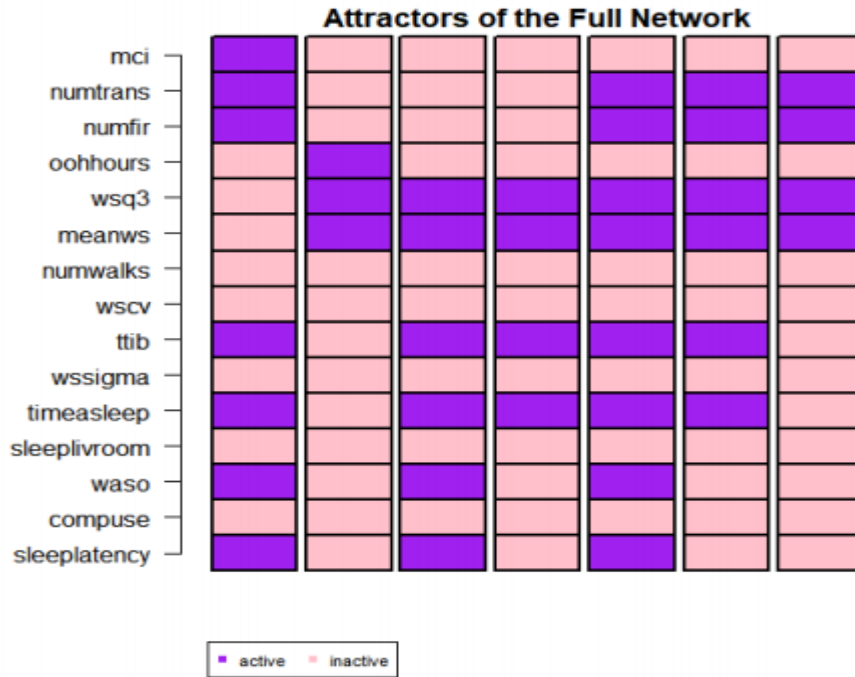


Figure 3: Attractors of the Full Life Kinetics and Impairment Network

The state transition graph of the steady states (attractors) of the reduced network is given in Figure 5. Analysis of the steady states and its basins were done using Pyboolnet (Klarner et. al., 2017). and Boolnet (Mussel, et. al., 2010). The seventh attractor in Figure 3 is an important attractor of the full and reduced network. It has a basin of 24064 weak attractors, while the strong and cycle-free attractors have basins of 2048 states each for an asynchronous update scheme of the full network. The fourth attractor has a basin of 15360 weak attractors, while the strong and cycle-free attractors have 64 states each. The third attractor has a basin containing 13344 weak attractors, with 64 and states each that are cycle-free and strong respectively. The second attractor has a weak basin of 18432 weak attractors,

while the cycle-free and strong basins are both 256 states each.

Attractor	Basin size (weak)	Basin size (strong and cycle-free)
1	13824 states	128 states each
2	18432 states	256 states each
3	13344 states	64 states each
4	15360 states	64 states each
5	17376 states	128 states each
6	20096 states	512 states each
7 (last)	24064 states	2048 states each

Table 1: Basin sizes of attractors

The sixth attractor has a weak basin of 20096 weak attractors, with strong and cycle-free basins of 512 states each.

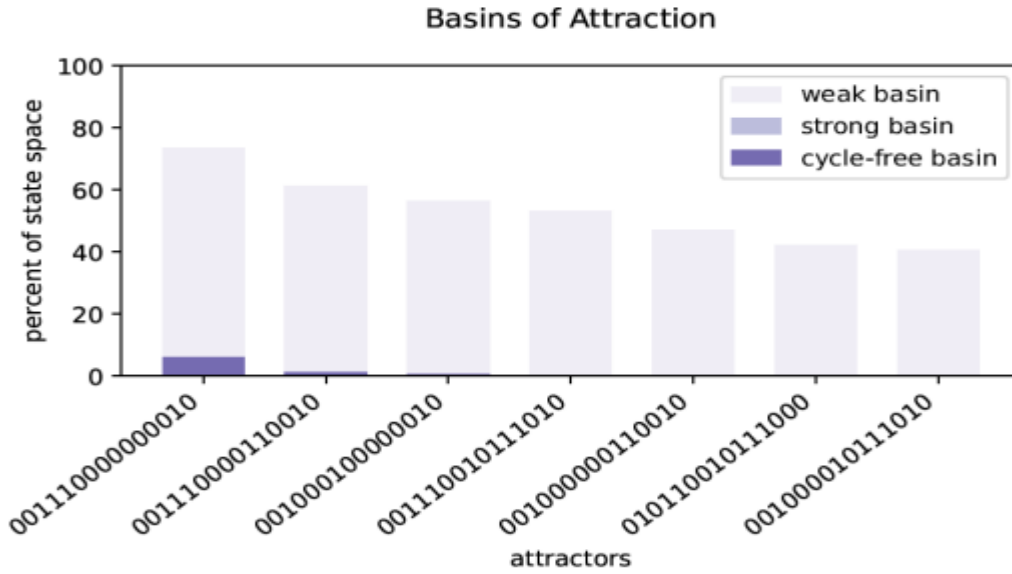


Figure 4: Basins of Attraction of the Full Network (Parameters are encoded in the order : {compuse, mci, meanws, numfir, numtrans, numwalks, oohhours, sleep latency, sleepivroom, time asleep, ttib, waso, wscv, wsq3, wssigma})

The fifth attractor has a weak basin of 17376 weak attractors, with cycle-free and strong basins of 128 states each. The first attractor which happens to be the only attractor with $mci = 1$, has a weak basin of 13824 weak attractors and also cycle-free and strong basins with the same size as the fifth attractor (see Figure 4). The analysis of the basin of attraction of the reduced

network is given in Figure 8 that contains a bar chart of all attractors, their percentage of state space and basin type, the Figure 6 shows the pie chart of the basins of attraction for each attractors of the reduced network and their overall percentage in the state space of the strong basin of attraction.



Figure 5: State transition graph of the reduced Life kinetics and Impairment Network (Parameters are encoded in the following order: {mci, meanws, numfir, ttib, waso, wscv})

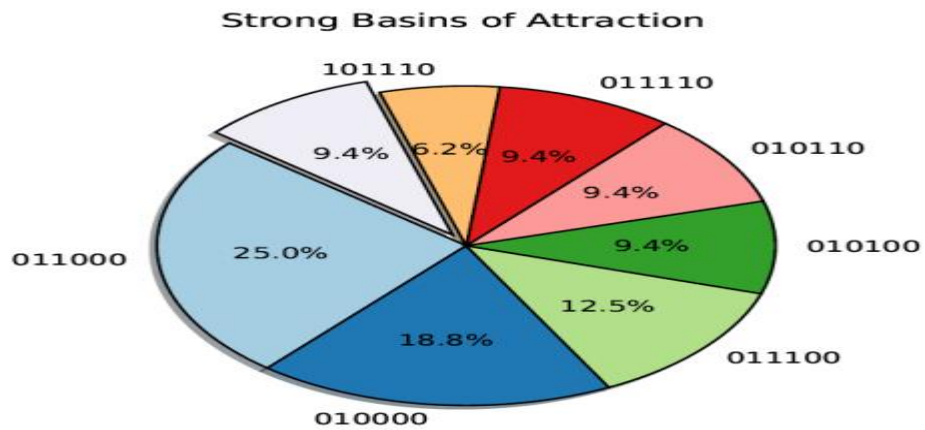


Figure 6: Pie chart of the state space of the strong basin of attraction of the reduced network

However, limitations existed in characterizing dynamic responses. By analyzing the attractor landscape in this section, a more comprehensive view of the network's dynamic capabilities and limitations was obtained. Specifically,

identifying control targets that can switch the network between attractors provides insight into potential intervention strategies for changing dysfunctional behaviors (Samaga, et al, 2009).

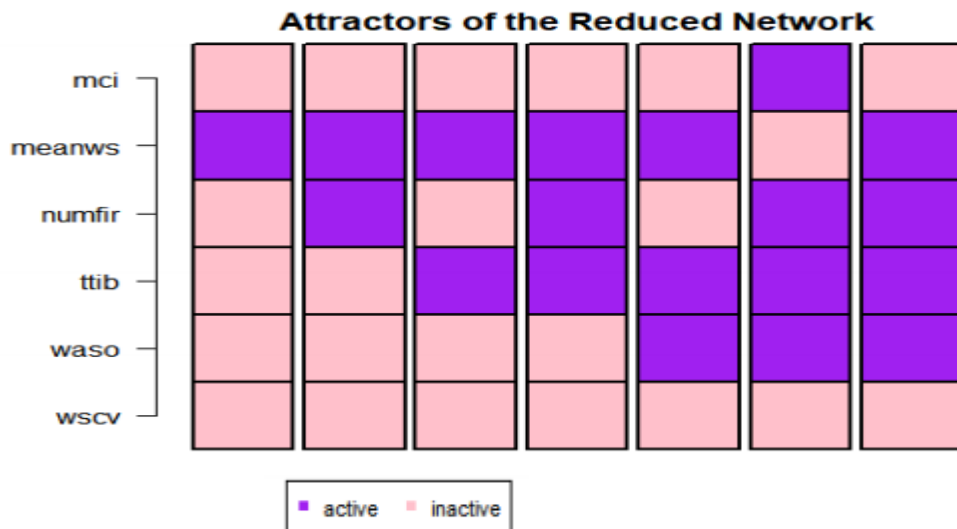


Figure 7: Attractors of the Reduced Life Kinetics and Impairment Network

By setting the control intervention parameter to 0, control targets corresponding to endogenous network interactions were determined. This

revealed which existing connections in the network, if perturbed, could alter the systemic state in a desired way (Moser et. al., 2018).

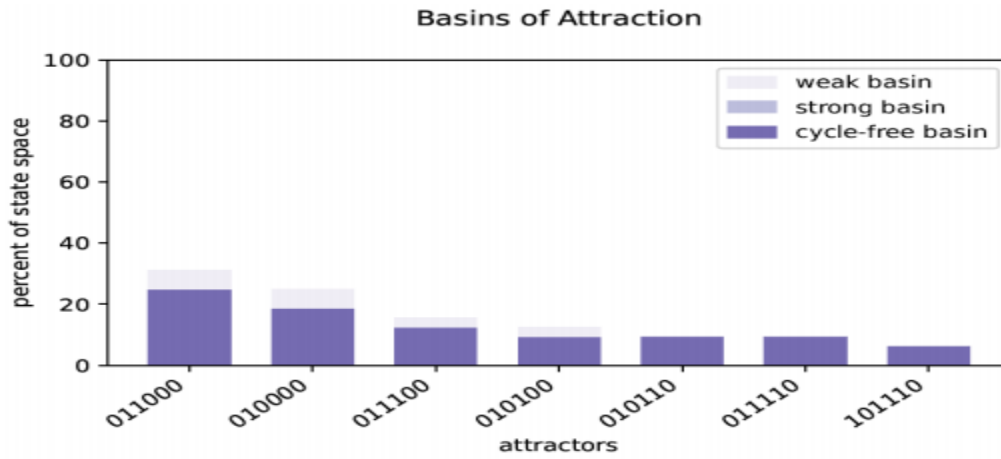


Figure 8: Basins of attraction of the reduced network and their state spaces

The images showing some of the control set for control targets ($mci = 0$), are given

in Figure 9 and Figure 10 for the full and reduced network respectively.

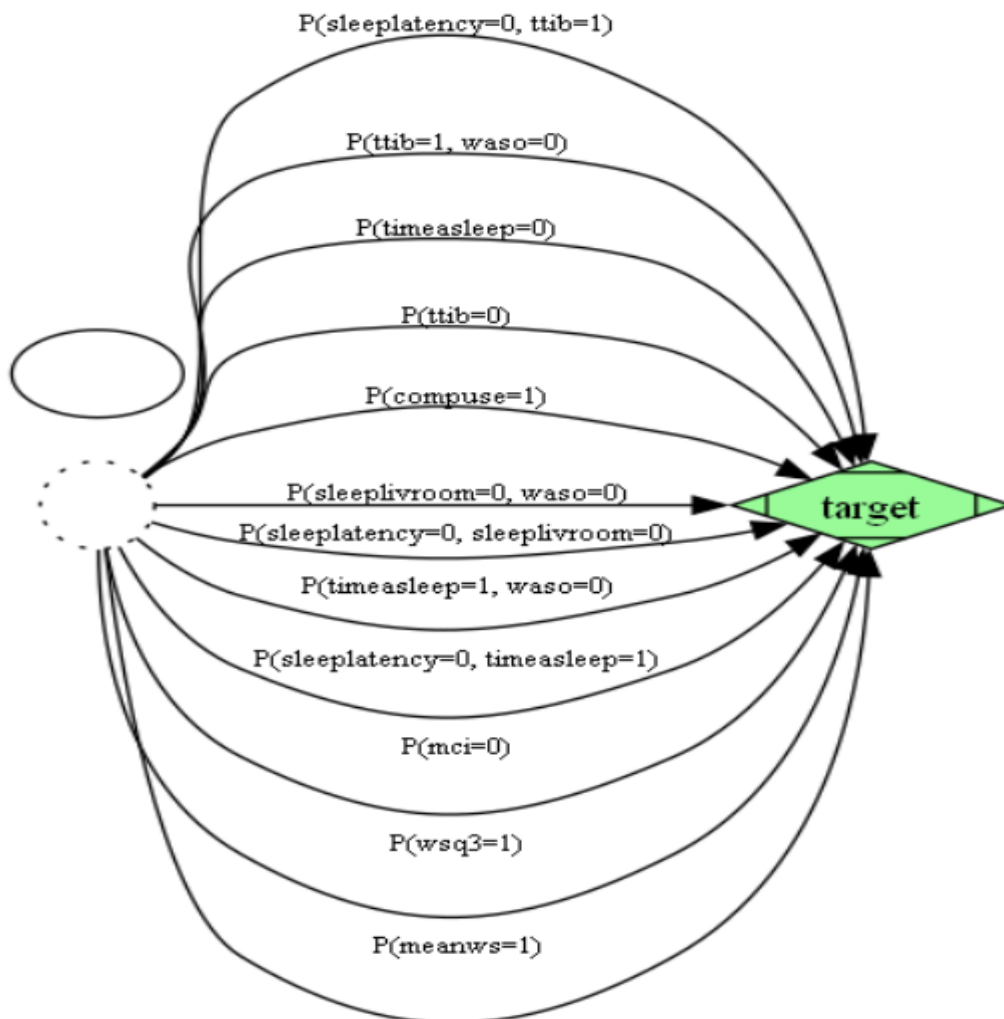


Figure 9: The control set for at most two (2) drivers for the Full reconstructed life kinetics and impairment network with control target $mci = 0$

Other control sets of the full network of more than two (2) drivers includes $\{ 'meanws': 0, 'waso': 0, 'ttib': 1 \}$, $\{ 'wsq3': 0, 'timeasleep': 1, 'sleeplatency': 0 \}$, $\{ 'wscv': 0, 'waso': 0, 'timeasleep': 1 \}$, $\{ 'timeasleep': 1, 'wsq3': 0, 'meanws': 0, 'sleeplatency': 0 \}$, $\{ 'wsq3':$

$0, 'sleeplatency': 0, 'timeasleep': 1, 'sleeplivroom': 1, 'ttib': 0 \}$. The overall results from this analysis provide a roadmap for potential therapies that modulate the network's natural dynamics (Steuer et. al., 2006).

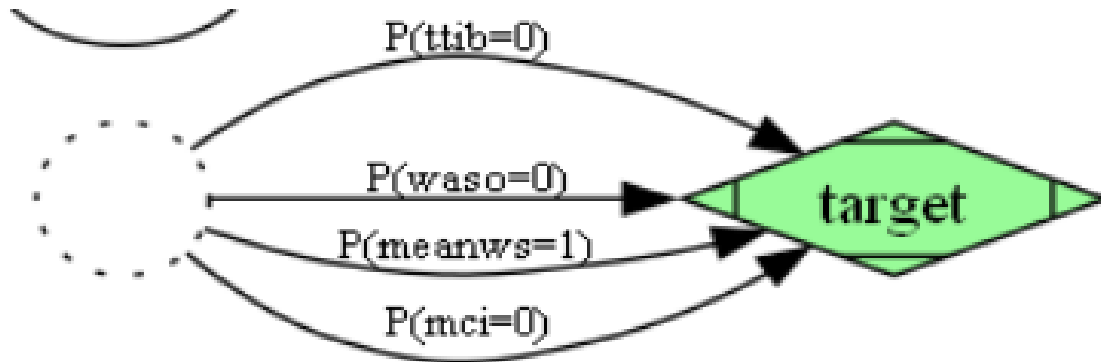


Figure 10: The control set for the Reduced reconstructed life kinetics and impairment network with control target $mci = 0$

However, it's important to note that identifying control targets in the full and reduced network is just the first step in developing effective interventions for MCI. Further experimental studies are needed to validate the effectiveness and safety of these interventions. Overall, identifying control targets in the networks can be a promising approach for developing interventions for MCI. By targeting specific nodes within the network, we can potentially shift the system's dynamics towards a healthier state, providing new avenues for treating this debilitating condition.

3. RESULT AND DISCUSSION

The target control analysis yielded several potential control targets in the reduced network whose modulation could modify MCI-associated attractors, demonstrating preservation of relevant dynamical features despite network reduction (see Materials and Methods). These findings corroborate research demonstrating that network reduction techniques can preserve attractor dynamics important for modeling

phenotype of interest (Shreim et. al., 2010) and (Qiu et. al., 2021).

In the full network, 16 control sets that fixed $mci=0$ was identified, suggesting regulation of those nodes could modulate MCI states. While fewer control targets were found in the reduced network (4 sets), the ability to still find interventions demonstrates preservation of essential dynamical features (Veliz-Cuba et al, 2014).

These includes;

- 1) 'waso': 0: This control set indicates that lowering the value of the 'waso' node could switch the network attractor from an MCI-associated state to a non-MCI state. 'waso' likely represents time awake after sleep onset, a measure of sleep consolidation and efficiency. Decreasing 'waso' by promoting more consolidated sleep may help prevent MCI onset by optimizing sleep-dependent memory and cognitive processes. However, further research is needed to determine whether directly reducing 'waso'

*Corresponding author, e-mail:ugbene.ifeanyi@fupre.edu.ng

- levels in patients is feasible and effective mitigating MCI.
- 2) 'ttib': 0: Fixing 'ttib' to 0 suggests that decreasing the value of the 'ttib' node could modulate MCI-associated attractors. 'ttib' likely denotes total time in bed, another sleep metric. Reducing 'ttib' by maintaining an optimized sleep duration may promote sleep efficiency and potentially counteract processes contributing to MCI. But rigorous experimental validation is essential to evaluate this computational prediction and determine whether interventions targeting 'ttib' could translate to physiological effects.
 - 3) 'meanws': 1: Increasing 'meanws' to 1 indicates that enhancing the value of the 'meanws' node may regulate MCI attractors. 'meanws' plausibly represents average walking speed, a measure of 15 motor function. Improving 'meanws' by promoting mobility may help compensate for processes underlying MCI. However, the precise identities and relationships of these network nodes remain unknown without wet lab experimentation to validate their physiological relevance.
 - 4) 'ttib': 1, 'sleeplatency': 0: Maintaining an optimal total time in bed while decreasing sleep latency may enhance sleep efficiency and continuity, potentially mitigating MCI. However, experimental validation is needed.
 - 5) 'waso': 0, 'ttib': 1: Decreasing time awake after sleep onset while maintaining an optimized total time in bed may improve sleep maintenance, aiding sleep-dependent processes that could mitigate MCI. But further research is required.
 - 6) 'timeasleep': 1, 'sleeplatency': 0: Fixing total sleep time at an optimized duration while decreasing sleep latency could regulate MCI attractors by promoting sleep optimization. However, experimental work is needed to define an appropriate value for 'timeasleep'.
 - 7) 'timeasleep': 1, 'waso': 0: Decreasing time awake after sleep onset while fixing total sleep time at an optimized duration may reflect enforcing consolidated sleep. This could theoretically mitigate MCI symptoms by optimizing sleep. But experimentally validating and translating these predictions into interventions requires more work.
 - 8) 'meanws': 1, 'numfir': 0: Increasing average walking speed while decreasing sensor firings in the home may reflect promoting mobility and reducing sedentary behavior. This could theoretically counteract processes underlying MCI. However, validation is required.
 - 9) 'meanws': 0, 'waso': 0, 'ttib': 1: Decreasing average walking speed while decreasing time awake after sleep onset and maintaining an optimized total time in bed may reflect promoting rest through limiting mobility and optimizing sleep. This could theoretically mitigate MCI symptoms, though experimental validation is needed.
 - 10) 'wsq3': 0, 'timeasleep': 1, 'sleeplatency': 0: Decreasing upper quartile of walking speed while fixings total sleep time at an optimized duration and decreasing sleep latency may reflect limiting higher-intensity activity while promoting basic sleep optimization. This could help mitigate MCI in sedentary individuals, though rigorous testing would be required.
 - 11) 'wscv': 0, 'waso': 0, 'timeasleep': 1: Decreasing variation in walking speed while decreasing time awake after sleep onset and fixing total sleep time at an optimized duration may reflect enforcing consistent activity at a basic

level while promoting sleep consolidation for a set duration. This could theoretically aid those with MCI, though experimental validation is ultimately needed.

12) 'timeasleep': 1, 'wsq3': 0, 'meanws': 0, 'sleeplatency': 0: Decreasing average and upper quartile walking speed while maintaining optimized total sleep time and decreasing sleep latency may reflect limiting mobility and activities while promoting sleep optimization. This restorative approach could potentially mitigate MCI symptoms, but requires rigorous testing and refining in experimental settings.

13) 'wsq3': 0, 'sleeplatency': 0, 'timeasleep': 1, 'sleeplivroom': 1, 'ttib': 0: Decreasing upper quartile walking speed, while fixings total sleep time in the living room and reducing sleep latency may reflect curtailing intense activity while promoting basic sleep optimization. The impact of sleep location remains undefined, emphasizing need for experimental validation and refinement of these putative control targets for MCI therapy.

14) 'compuse': 1: Fixing computer use at an optimized level may reflect leveraging technology in a regulated manner to compensate for cognitive declines in MCI. However, the specific identity and real-world impacts of this node require experimental validation. Further research is needed to determine whether and how optimizing technology engagement could meaningfully impact MCI symptoms in patients.

15) 'sleeplivroom': 0, 'sleeplatency': 0: Decreasing time asleep in the living room while also decreasing sleep latency may reflect enforcing a

regulated sleep schedule in the bedroom to promote sleep optimization. Sleeping in a dedicated bedroom has been associated with better sleep quality and continuity. However, experimental testing is ultimately needed to determine whether these dynamical changes could indeed regulate MCI associated attractors as predicted.

16) 'wsq3': 1: Increasing the upper quartile of walking speed may reflect promoting higher-intensity activity to counteract sedentary tendencies that could contribute to MCI progression. However, determining appropriate ways to implement this change and whether it could indeed regulate MCI associated attractors requires experimental validation.

The reduced network's size conferred a computational advantage, requiring 2.8x less time to identify controls. This trade-off between fidelity and efficiency is typical of network reduction (Qiu et. al., 2021). The potential control targets in the reduced network- 'waso', 'ttib', and 'meanws' - warrant rigorous experimental validation to test their ability to regulate MCI-associated attractors in vivo. Studies have shown in silico predictions of controls can translate to physiological modulation of disease dynamics (Chen et. al., 2020). However, research is needed to fully evaluate interactions, mechanisms and confounds (Chen et. al., 2020).

If validated, mechanistically altering these proposed targets- e.g. via drugs altering 'waso' levels, stimulation of nodes correlated with 'ttib' - could provide novel MCI treatment strategies by switching abnormal attractor states (Chen et. al., 2020). Network-based approaches increasingly contribute control candidates (Zhang et. al., 2008).

However, limitations remain. In silico predictions often oversimplify biology

(Zhang et. al., 2008). Incorporating lost network details post-reduction may improve fidelity. Alternative reduction methods preserving different features could identify distinct controls (Shreim et. al., 2010). Comparing predictions may converge on robust interventions (Shreim et. al., 2010). Impacts on off-target dynamics must be considered to avoid adverse effects (Chen et. al., 2020).

In summary, while network reduction preserved dynamical relevance for identifying potential MCI control targets, rigorous experimental validation is needed. Comparisons across methods, incorporation of lost details, and evaluation of non-target impacts may inform selection of optimal strategies. Dynamics-based approaches hold promise for iteratively refining predictions through experiment modeling cycles (Zhang et. al., 2008). Network reduction may ultimately help create tailored interventions for complex conditions like MCI (Wang et. al., 2012).

4. CONCLUSION

In conclusion, our research demonstrates the potential of network reduction techniques for modeling and regulating complex conditions such as MCI. By identifying control targets within Boolean molecular network models through computational algebra, we have identified key parameters that can be targeted for intervention. Our analysis of the full network and reduced network models revealed that the parameters most strongly associated with MCI were *meanws*, *ttib*, and *waso*. While our study provides valuable insights into potential control targets for regulating MCI, there are several limitations that must be acknowledged. Our analysis was limited to a Boolean molecular network model, and future studies should explore the use of other modeling techniques. Additionally, our study was based on a small sample

size, and further research is needed to validate our findings in larger populations.

Looking ahead, our research highlights several avenues for future work. Further studies could explore the use of network reduction techniques in other complex conditions and investigate the effectiveness of targeting the identified control targets. Additionally, future studies could explore the use of more sophisticated modeling techniques to better capture the complexities of biological systems. Overall, our research emphasizes the potential impact of network reduction for modeling and regulating complex conditions like MCI. By identifying key control targets, these techniques can provide valuable insights into potential interventions for these conditions.

References

- Albert R. and Othmer H. G. (2003), The topology of the regulatory interactions predicts the expression pattern of the segment polarity genes in *Drosophila melanogaster*. *Journal of Theoretical Biology*, 223(1), 1 – 18.
- Chen, S., Bowman, F. D., and Xing, Y. (2020). Detecting and Testing Altered Brain Connectivity Networks with K-partite Network Topology. *Computational statistics & data analysis*, 141, 109–122. <https://doi.org/10.1016/j.csda.2019.06.007>
- Choi M., Shi J., Jung S. H., Chen X., and Cho K. H. (2012). Attractor landscape analysis reveals feedback loops in the p53 network that controls the cellular response to DNA damage. *Science Signaling*. 2012;5(251), ra83. <https://doi.org/10.1126/scisignal.2003363>
- Cox D, Little J, and O'shea D. (1998), *Using algebraic geometry*, volume

- 185 of Graduate Texts in Mathematics. New York: Springer-Verlag.
- Dinwoodie, Ian H., (2016). Computational Methods for Asynchronous Basins". Mathematics and Statistics Faculty Publications and Presentations. 164.
- Gunawardena, J. (2010). Models in Systems Biology: The Parameter Problem and the Meanings of Robustness. In H. M. Lodhi & S. H. Muggleton (Eds.), *Elements of Computational Systems Biology* (pp. 19-47). DOI: 10.1002/9780470556757.ch2.
- Huang S. (1999), Gene expression profiling, genetic networks, and cellular states: an integrating concept for tumorigenesis and drug discovery. *Journal of molecular Medicine (Berlin)*, 77(6): 469–480.
- Kauffman S. A. (1969), Metabolic stability and epigenesis in randomly constructed genetic nets. *J Theor Biol.*; 22(3):437– 467.
- Kaye J. A., Maxwell S. A., Mattek N, Hayes T. L., Dodge H., Pavel M., Jimison H. B., Wild K., Boise L., and Zitzelberger T. A. (2011), Intelligent systems for assessing aging changes: home-based, unobtrusive, and continuous assessment of ageing. *The Journals of Gerontology, Series B: Psychological Sciences and Social Sciences*, 66B(S1), i180-i190.
- Klärner, H., Streck, A., and Siebert, H. (2017). PyBoolNet: a python package for the generation, analysis and visualization of boolean networks. *Bioinformatics (Oxford, England)*, 33(5), 770–772. <https://doi.org/10.1093/bioinformatics/btw682>
- Moser, F., Espah Borujeni, A., Ghodasara, A. N., Cameron, E., Park, Y., and Voigt, C. A. (2018). Dynamic control of endogenous metabolism with combinatorial logic circuits. *Molecular systems biology*, 14(11), e8605. <https://doi.org/10.15252/msb.20188605>
- Mussel, C., Hopfensitz, M., & Kestler, H. A. (2010). BoolNet—an R package for generation, reconstruction and analysis of Boolean networks. *Bioinformatics*, 26(10) 1378–1380. <https://doi.org/10.1093/bioinformatics/btq124>
- Qiu, L., Zhang, J., Tian, X., and Zhang, S. (2021). Identifying Influential Nodes in Complex Networks Based on Neighborhood Entropy Centrality. *The Computer Journal*, 64(10), 1465–1476. <https://doi.org/10.1093/comjnl/bxab034>
- Rozum, J. C., Deritei, D., Park, K. H., Zanudo, J. G. T., and Albert, R. (2022). pystablemotifs: Python library for attractor identification and control in Boolean networks. *Bioinformatics*, 38(5), 1465–1466. <https://doi.org/10.1093/bioinformatics/btab825>
- Saadatpour, A., Albert, I., and Albert, R. (2010). Attractor analysis of asynchronous Boolean models of signal transduction networks. *Journal of Theoretical Biology*, 266(4), 641-656.
- SageMath. (Version 9.2) [Computer software]. (2021). Available from <http://www.sagemath.org>.
- Samaga, R., Saez-Rodriguez, J., Alexopoulos, L. G., Sorger, P. K., and Klamt, S. (2009). The logic of EGFR/ErbB signaling: theoretical properties and analysis of high-throughput data. *PLoS computational biology*, 5(8), e1000438. <https://doi.org/10.1371/journal.pcbi.1000438>
- Schwab J. B., Ikonomi, N., Werle, S. D., Weidner, F. M., Geiger, H., & Kestler, H. A. (2021), Reconstructing Boolean network

- ensembles from single-cell data for unraveling dynamics in the aging of human hematopoietic stem cells. *Computational and Structural Biotechnology Journal*, 19, 5321 – 5332.
<https://doi.org/10.1016/j.csbj.2021.09.012>
- Shmulevich, I., Dougherty, E. R., Kim, S., and Zhang, W. (2002). Probabilistic Boolean Networks: a rule-based uncertainty model for gene regulatory networks. *Bioinformatics (Oxford, England)*, 18(2), 261–274.
<https://doi.org/10.1093/bioinformatics/18.2.261>
- Shreim, A., Berdahl, A., Greil, F., Davidsen, J., and Paczuski, M. (2010). Attractor and basin entropies of random Boolean networks under asynchronous stochastic update. *Physical Review E*, 82(3), 035102(R)
- Steuer R, Kurths J., Fiehn O., & Weckwerth, W. (2003) Observing and interpreting correlations in metabolomics networks. *Bioinformatics* 19(8), 1019 – 1026.
<https://doi.org/10.1093/bioinformatics/btg120>
- Strogatz S. H. (2001) Exploring complex networks. *Nature*.;410(6825): 268–276.
<https://doi.org/10.1038/35065725>
- Veliz-Cuba A, Aguilar B, Hinkelmann F, and Laubenbacher R. (2014), Steady state analysis of boolean molecular network models via model reduction and computational algebra. *BMC Bioinforma.*;15:221.
- Veliz-Cuba A, Jarrah A.S., Laubenbacher R. (2010), Polynomial algebra of discrete models in systems biology. *Bioinformatics*.;26(13):1637–43. doi:10.1093/bioinformatics/btq240.
- Videla, S., Saez-Rodriguez, J., Guziolowski, C., & Siegel, A. (2017). caspo: a toolbox for automated reasoning on the response of logical signaling networks families. *Bioinformatics (Oxford, England)*, 33(6), 947–950.
<https://doi.org/10.1093/bioinformatics/btw738>
- Zhang R, Shah M. V., Yang J., Nyland S. B., Liu X, Yun J. K., Albert R., and Loughran T. P. Jr. (2008). Network model of survival signaling in large granular lymphocyte leukemia. *Proceedings of the National Academy of Science USA*, 105(42) : 16308–13. doi:10.1073/pnas.0806447105.